Hindawi Publishing Corporation
EURASIP Journal on Wireless Communications and Networking
Volume 2008, Article ID 437801, 13 pages
doi:10.1155/2008/437801

Research Article

Power Backoff Reduction Techniques for Generalized Multicarrier Waveforms

F. Danilo-Lemoine,[1] D. Falconer,[1] C.-T. Lam,[1] M. Sabbaghian,[1] and K. Wesołowski[2]

[1] *Department of Systems and Computer Engineering, Carleton University, Ottawa, Canada K1S 5B6*
[2] *Institute of Electronics and Telecommunications, Poznań University of Technology, 60965 Poznań, Poland*

Correspondence should be addressed to D. Falconer, ddf@sce.carleton.ca

Received 3 April 2007; Revised 31 July 2007; Accepted 18 October 2007

Recommended by Hikmet Sari

Amplification of generalized multicarrier (GMC) signals by high-power amplifiers (HPAs) before transmission can result in undesirable out-of-band spectral components, necessitating power backoff, and low HPA efficiency. We evaluate variations of several peak-to-average power ratio (PAPR) reduction and HPA linearization techniques which were previously proposed for OFDM signals. Our main emphasis is on their applicability to the more general class of GMC signals, including serial modulation and DFT-precoded OFDM. Required power backoff is shown to depend on the type of signal transmitted, the specific HPA nonlinearity characteristic, and the spectrum mask which is imposed to limit adjacent channel interference. PAPR reduction and HPA linearization techniques are shown to be very effective when combined.

1. INTRODUCTION

High-power amplifiers (HPAs) used in radio transmitters have nonlinear characteristics which can cause significant distortion to signals whose instantaneous power fluctuations come too close to the HPAs output saturation power. Even small amounts of nonlinear distortion can cause undesirable spectral regrowth, which can interfere with signals in adjacent frequency channels. Transmitted spectra must generally be confined within spectral masks which are imposed by regulatory agencies to keep worst-case adjacent channel interference to acceptable limits. Larger amounts of nonlinear distortion also cause nonlinear in-band self-interference, which results in increased received bit error rate. Normally, HPAs are operated with a certain "power backoff" which can be defined as the ratio of maximum saturation output power to lower average output power. The larger the backoff is, the less the nonlinear distortion will be. However, for a given transmitted power, a larger power backoff lowers HPA efficiency and increases overall power consumption and battery drain. It also means that a more expensive HPA, with a higher maximum output power rating, is necessary to produce a given average output power. The HPA is generally one of the most significant cost components of user terminals, and the relationship of HPA cost to maximum power rating is an important technology issue. The cost can rise sharply with the output power rating, and it is affected not only by the HPA device itself but also by thermodynamics, that is, provision of heat sinks, fans, and so forth [1].

Minimizing power backoff is thus desirable, without sacrificing BER performance or spectral efficiency, especially for cost- and power-sensitive user terminals. Two main approaches are pursued, which can be applied singly or in combination: (1) peak-to-average power ratio (PAPR) reduction to reduce the dynamic range of the transmitted signal before it is applied to the HPA and (2) direct HPA predistortion to compensate for the HPA distortion. The requirements and methods are strongly dependent on the modulation and multiplexing schemes. For example, multicarrier or parallel modulation and multiplexing schemes, such as orthogonal frequency division multiplexing (OFDM) and multicarrier code division multiple access (MC-CDMA), have inherently higher PAPR value than single-carrier or serial schemes [2].

PAPR reduction schemes have been extensively studied for OFDM and other multicarrier signals (see, e.g., [3, 4] and the references therein). In this paper, we broaden the application of PAPR reduction and HPA predistortion techniques to a more general class of frequency domain-generated signals

known as generalized multicarrier (GMC) signals [5–7]. This class includes OFDM and frequency domain-generated single-carrier signals, as well as multicarrier signals with noncontiguous spectral occupancy. Rather than introducing significantly new PAPR reduction techniques, we focus on the spectral regrowth reduction that existing schemes and variations of them can achieve for important classes of GMC signals at the output of a realistic HPA. Previous analyses of spectral regrowth generally rely on power series expansions, with few terms, of HPA input/output characteristic models [8], but more general models, capable of representing a wide range of HPAs, are best accommodated by simulation of output power spectra. This is the approach we use in this paper.

This focus on spectral regrowth differentiates the paper from most of the previous papers, which tend to focus on PAPR distributions and/or receiver performance degradations due to nonlinear distortion. In practice, at power backoff levels for which significant spectral regrowth starts to become noticeable, bit error rate degradation due to the nonlinearity is small—a fact which will be illustrated by results shown in Section 4.

Section 2 reviews OFDM and the more general GMC signal classes. Section 3 provides a reference background by comparing transmitted waveform amplitude distributions and HPA output power spectra for OFDM and discrete Fourier transform—(DFT-) precoded GMC signals. Sections 4 and 5 consider clipping and filtering, and selective mapping techniques, respectively. GMC signals with noncontiguous data spectra are considered in Section 6, including signals with frequency-multiplexed pilots and interleaved frequency division multiple access (IFDMA), and block IFDMA signals. Section 7 describes an HPA predistortion technique that can be used in combination with PAPR reduction techniques. Finally, Section 8 contains summary and conclusions. Some of the variations of PAPR reduction and predistortion presented here have previously appeared in recent conference papers by the authors in [9–13]. This paper presents these and other results in a unifying context.

2. PAPR REDUCTION FOR OFDM AND OTHER GENERALIZED MULTICARRIER SIGNALS

A block OFDM signal, transmitting coded data symbols $\{A_m,\ m = 0, 1, \ldots, M\}$, is normally generated as the inverse discrete Fourier transform (DFT) of the data symbol sequence. The resulting *OFDM symbol*, sampled at $N \geq M$ times per block, is expressed as

$$s(n) = \frac{1}{\sqrt{M}} \sum_{m=0}^{M-1} A_m \exp\left(j \frac{2\pi mn}{N}\right), \quad n = 0, 1, \ldots, N-1. \tag{1}$$

To this end, the OFDM symbol is prepended by a cyclic prefix (CP), which is a copy of the last N' samples, where N' exceeds the maximum expected channel impulse response length. The CP is discarded at the receiver; its purpose is to prevent interblock interference and to impart a circular convolution structure to the received block, thus facilitating the use of DFT processing (normally implemented with fast Fourier transform (FFT)). Each such block in a sequence of blocks generated in this way is windowed by a rectangular function whose length is $N + N'$ samples; this would cause undesirable sinc function spectral sidelobes, decaying only inversely with frequency. For this reason, a smoother time window is normally applied, such as a raised-cosine window, for which the sidelobe decay is proportional to the inverse cube of frequency.

Any sample $s(n)$ is a linear combination of M data symbols, equally weighted in magnitude. Therefore, its maximum possible magnitude is at least M times the average data symbol magnitude. This ratio could be the basis for the peak-to-average power ratio (PAPR) definition, but it is not very useful since for large M, the peak magnitude is seldom achieved. Other measures reflecting signal magnitude variation are discussed in the next section.

Methods for PAPR reduction of OFDM signals include nonlinear block error correction coding [14, 15], selective mapping (SLM) [16], partial transmit sequences [16, 17], reference signal subtraction [3], and amplitude predistortion [18]. All of the above methods require extra transmitter signal processing complexity[1] and most of them also require the transmission of extra overhead. OFDM signals may also be clipped to remove power peaks, followed by filtering to suppress out-of-band spectral regrowth caused by the nonlinear clipping operation. Several stages of clipping and filtering are more effective than one since the filtering operation tends to restore some of the signal's peakedness [19–21]. This approach has the virtue that no extra processing or side information is necessary for reception, but it can cause a slight degradation in bit error rate due to the clipping-caused nonlinear distortion on the signal.

A more general form of OFDM signal format, called generalized multicarrier (GMC) [5–7], is formed by performing a matrix transformation on the vector $\mathbf{a}$ of M data symbols before applying (1):

$$\mathbf{A} = \mathbf{Ma}, \tag{2}$$

where $\mathbf{M}$ is an N by M matrix. The transmitted signal vector $\mathbf{s}$ can be expressed as

$$\mathbf{s} = \mathbf{F}^* \mathbf{Ma}, \tag{3}$$

where $\mathbf{F}^*$ is the N by N inverse DFT matrix.

Most linearly modulated signal types such as multicarrier code division multiple access (MC-CDMA) and interleaved frequency division multiple access (IFDMA) can be generated in this way, by the appropriate choice of $\mathbf{M}$. Choosing $\mathbf{M}$ as an identity matrix gives OFDM. Inserting rows of zeroes in the identity matrix gives orthogonal frequency division multiple access (OFDMA), in which data-bearing subcarriers are selected based on diversity or traffic considerations.

[1] Typically, these methods require generation and comparisons, on the basis of PAPR, of several possible versions of the same transmitted waveform, and selection of the one with the lowest peak value.

A version of GMC, which is of interest in this paper, is *DFT-precoded OFDM*,[2] in which **M** contains a DFT matrix, that is,

$$\mathbf{M} = \begin{bmatrix} \mathbf{F} \\ \mathbf{0} \end{bmatrix}, \tag{4}$$

where **F** is an M by M DFT matrix, whose mnth element is $(1/\sqrt{M})e^{-j2\pi(mn/M)}$ for $0 \le m, n \le M-1$, and **0** is an $(N-M)$ by M matrix of zeroes. Combining (4) and (3) yields the expression for the sampled waveform:

$$s(n) = \sum_{m=0}^{M-1} a_m\, g\left(n - m\frac{N}{M}\right), \quad n = 0, 1, \ldots, N-1, \tag{5}$$

where

$$g(n) = \frac{1}{M} e^{j(\pi/N)(M-1)n} \frac{\sin(\pi M/N)n}{\sin(\pi/N)n}. \tag{6}$$

This describes samples of *serial modulated* (SM) or *single-carrier* (SC) waveform, in which data symbols are transmitted serially, at intervals of N/M samples by pulse amplitude modulating a pulse waveform $g(n)$. Here, $g(n)$ is a circularly shifted, sampled version of a band-limited pulse waveform with zero excess bandwidth (or zero rolloff); it is time-limited to N samples. Its envelope decays approximately as n^{-1}. Thus, the magnitude of each sample $s(n)$ is mainly determined by a weighted sum of a small number of adjacent data symbols, and so, as with any SM waveform, its dynamic range will be much less than that of the equivalent OFDM waveform. The amplitude range of $s(n)$ can be further reduced, at the expense of increasing the signal bandwidth, by replacing $g(n)$ by a circularly shifted raised cosine or other pulse with excess bandwidth. Another variant of DFT-precoded OFDM, with similar low-PAPR properties, is interleaved frequency division multiple access (IFDMA),[3] in which L rows of zeroes are inserted after every row of **F** in (4) [22]. The signal spectrum then consists of M DFT-modulated subcarriers at intervals of L. The pulse $g(n)$ can then be shown to be that of (6), but with n being replaced by Ln. Thus, IFDMA produces a serial modulated signal. IFDMA has the advantage over contiguous-spectrum signals of extra frequency diversity since its spectrum is spread over a wider band. Another recently proposed variation is block IFDMA (B-IFDMA), in which subcarriers are grouped in small blocks, well separated from other blocks [23] to enhance frequency diversity. In contrast to IFDMA, B-IFDMA does not result in a pure serial modulation waveform, but it is shown in [23] and in Section 6 that it still has good PAPR and power backoff properties.

[2] This is also called localized SC-FDMA in the context of 3GPP long-term evolution.

[3] IFDMA is also called distributed SC-FDMA in the context of 3GPP long-term evolution.

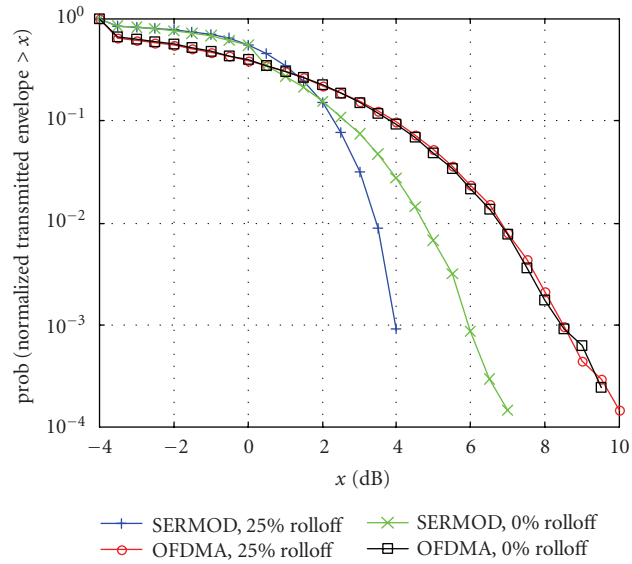

Figure 1: Distribution of instantaneous power for comparable OFDMA and serial modulated waveforms with 0% rolloff, generated in the frequency domain with 5.5% raised-cosine *time-domain* windowing, and with 25% rolloff generated in the time domain by square-root raised-cosine *frequency domain* filtering. The number of data symbols per block is $M = 256$.

3. PAPR AND SPECTRAL REGROWTH AT HPA OUTPUT

PAPR is a commonly used measure of the range of a signal's amplitude. It is a reasonably good *qualitative* measure; signals with low PAPR generally require less power backoff and exhibit less performance sensitivity when amplified by a nonlinear HPA than do signals with high PAPR. However, PAPR is determined by the single largest-amplitude sample in a block of N samples, and therefore it is not a good *quantitative* measure of nonlinearity sensitivity. Somewhat more informative is the complementary cumulative distribution (CCDF) function of the signal amplitude measured over many samples. Figure 1 illustrates CCDFs of QPSK serial modulated and OFDMA signals generated by (a) the zero rolloff frequency domain method of (4)–(6), with a number of used subcarriers $M = 256$ and 5.5% raised-cosine windowing of the time-domain waveform, and (b) the traditional time-domain method, with 25% excess bandwidth square-root raised-cosine filtering of the time-domain waveform, again with 256 symbols per block. The lower amplitude range of the serial modulated (or DFT-precoded OFDM) signal is evident. It is also evident that excess bandwidth (25% versus 0%) reduces the amplitude range of the serial modulation signal, because of lower $g(n)$ sidelobes, while having little or no effect on the OFDM signal's amplitude range.

However, the CCDF does not provide quantitative information about sensitivity to specific HPA nonlinearities. Such information is available from the simulation of nonlinear amplification of waveforms, using realistic power amplifier models and measuring output power spectra and signal-to-distortion ratios. An Rapp model [24] (see Figure 2),

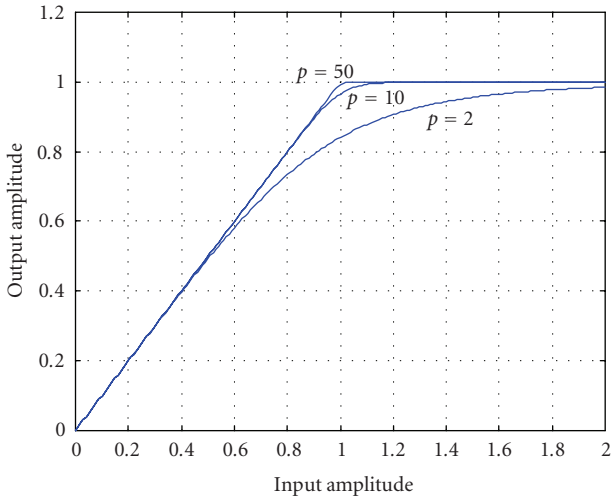

Figure 2: Rapp model of HPA nonlinearity.

with a parameter $p = 2$, is a good approximation to the amplitude-to-amplitude conversion characteristic of a typical low-cost solid-state power amplifier. The ratio of output to input amplitude in this model with parameter p is given by

$$\left| \frac{V_{\text{out}}}{V_{\text{in}}} \right| = \frac{1}{\left[1 + |V_{\text{in}}/V_{\text{sat}}|^{2p}\right]^{1/(2p)}}, \tag{7}$$

where V_{sat} is the saturated output level of the amplifier.[4] With $p = 10$ or higher, the characteristic approaches that of an ideal linear clipper. Examples of spectral regrowth due to a $p = 2$ nonlinearity for the OFDM and serial modulated QPSK signals of Figure 1 are shown in Figures 3(a) and 3(b). The greater the power backoff is—which can be defined as the ratio of maximum saturation output power to actual average output power—the less the spectral regrowth at the HPA output will be. In Figure 3 and most subsequent power spectra figures, the average signal powers of signals being compared (and hence their backoffs) are adjusted so that their resulting output power spectra are very similar, in order that they barely satisfy the same imposed spectral mask. Figure 3(a) shows that for the 0% rolloff frequency domain-generated signals, whose CCDFs are shown in Figure 1, serial modulation and OFDM require 7 dB and 9 dB backoffs, respectively, for comparable maximum spectrum sidelobe levels of about −40 dB. The backoff for serial modulation is further decreased to about 6.3 dB for the time-domain-generated signals with 25% rolloff although the signals' bandwidth has increased by 25% with this rolloff factor.

The required power backoff is significantly reduced by up to 2–4 dB for an HPA with Rapp parameter $p = 10$ that approximates an ideal linear clipper, as shown in Figures 4(a) and 4(b) for the same signals as in the previous figures. This is an indication, which will be reinforced by later examples, that linearization by predistortion of the HPA characteristic (as proposed in Section 7) is a very useful complement to PAPR reduction techniques for reducing the required power backoff.

For small values of p the out-of-band radiation has smaller components at higher frequencies and most of the out-of-band power is concentrated in the near in-band spectrum. On the other hand, for large p, the out-of-band radiation components are spread over a wider frequency range. This can be seen if we use the binomial expansion for the denominator of the Rapp model. The expansion of the Rapp model would be

$$V_{\text{out}}(t) = \begin{cases} V_{\text{in}}(t) + \sum_{k=1}^{\infty} \widetilde{a}_k [V_{\text{in}}(t)]^{2pk+1}, & V_{\text{in}}(t) < V_{\text{sat}}, \\ V_{\text{sat}} + \sum_{k=1}^{\infty} \widetilde{b}_k [V_{\text{in}}(t)]^{-2pk}, & V_{\text{in}}(t) < V_{\text{sat}}, \end{cases} \tag{8}$$

where $\widetilde{a}_k = (r)_k V_{\text{sat}}^{-2pk}$, $\widetilde{b}_k = (r)_k V_{\text{sat}}^{2pk}$, $r = -1/2p$, and $(r)_k$ is the Pochhammer symbol:

$$(r)_k = \frac{\Gamma(r+k)}{\Gamma(r)} = (r+k-1), \ldots, (r+1)r. \tag{9}$$

If we assume that the saturation level is high enough to use only the first formula for $V_{\text{in}} < V_{\text{sat}}$ and compare the out-of-band radiation of amplifiers with two different values of p, the corresponding outputs for $p = 2$ and $p = 10$ would be

$$\begin{aligned} V_{\text{out},p=2} &= V_{\text{in}}(t) + (r)_1 V_{\text{sat}}^{-4} V_{\text{in}}(t)^5 + (r)_2 V_{\text{sat}}^{-8} V_{\text{in}}(t)^9 + \cdots, \\ V_{\text{out},p=10} &= V_{\text{in}}(t) + (r)_1 V_{\text{sat}}^{-20} V_{\text{in}}(t)^{21} + (r)_2 V_{\text{sat}}^{-40} V_{\text{in}}(t)^{41} + \cdots. \end{aligned} \tag{10}$$

The expansion of the output when $p = 2$ includes smaller powers of the input signal. Thus, for $p = 2$, the out-of-band radiation power is more concentrated at frequencies closer to the in-band spectrum. The second term of the above expansion generates the major part of the distortion. When $p = 2$, this term is larger than when $p = 10$. This increases the adjacent out-of-band radiation of the amplifier with $p = 2$ relative to that with $p = 10$.

Figures such as 3 and 4, showing HPA output power spectra for typical nonlinearity models, clearly provide more useful quantitative information on required power backoffs than do PAPR or CCDF results, such as in Figure 1. At the levels of spectral regrowth shown in Figures 3 and 4 (which conform to typical spectral mask requirements), the received in-band signal-to-nonlinear distortion ratios are quite small: in the order of 35 to 40 dB. In general, we find that the spectral regrowth allowed by typical spectral masks is the dominating criterion for HPA nonlinearity effects. In-band nonlinear distortion and bit error rate degradation of the received signal are negligible at backoff values that start to impinge on typical spectral masks, as will be illustrated in the next section.

[4] In this formula, the amplifier gain is normalized to unity for notational convenience.

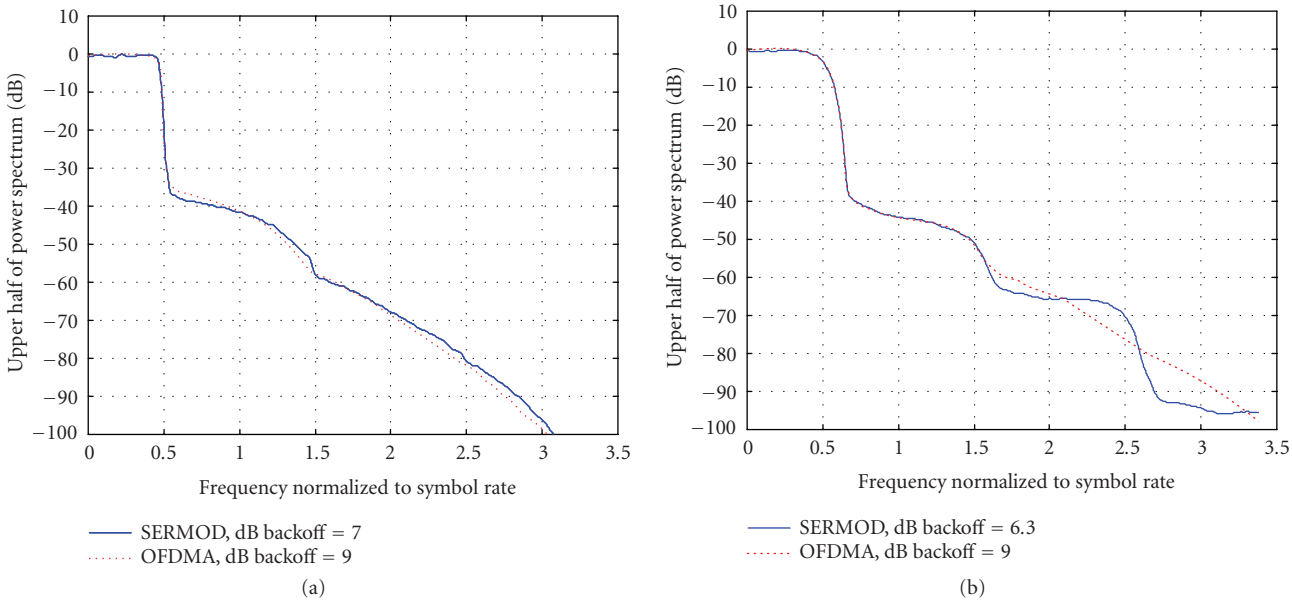

FIGURE 3: Power spectra at output of a $p = 2$ Rapp nonlinearity for QPSK OFDM and serial modulated signals with (a) 0% and (b) 25% excess bandwidths.

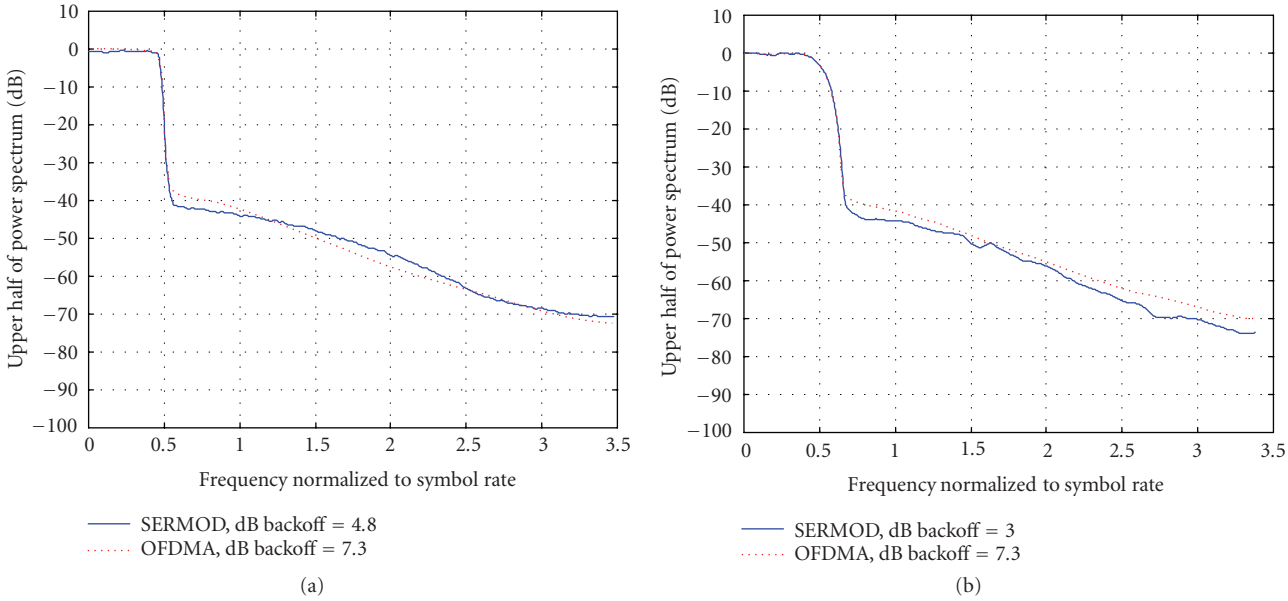

FIGURE 4: Power spectra at output of a $p = 10$ Rapp nonlinearity for QPSK OFDM and serial modulated signals with (a) 0% and (b) 25% excess bandwidths.

4. CLIPPING AND FILTERING

It is well known that the dynamic range of the instantaneous power of OFDM signals can be reduced by a variety of techniques mentioned above. It is perhaps not so well appreciated that many of these techniques can also be applied to DFT-precoded OFDM or serial modulation. Even clipping and filtering (see [19, 20] and the references therein) can be applied to serial modulation, as to OFDM, with only moderate effects of nonlinear distortion on the received signal. An example of the effect of one stage of clipping and filtering, on bit error probability of 16 QAM serial modulation signal in additive white Gaussian noise, for various degrees of power backoff, is shown in Figure 5. The clip level equals the amplifier saturation level. The BER performance is seen to be relatively robust to clipping and filtering and the nonlinear amplifier for backoffs down to 5 dB, especially for $p = 10$.

Several iterations of clipping and filtering, as described in [20], can be applied to frequency domain-generated serial modulated and OFDMA signals. Examples of spectral

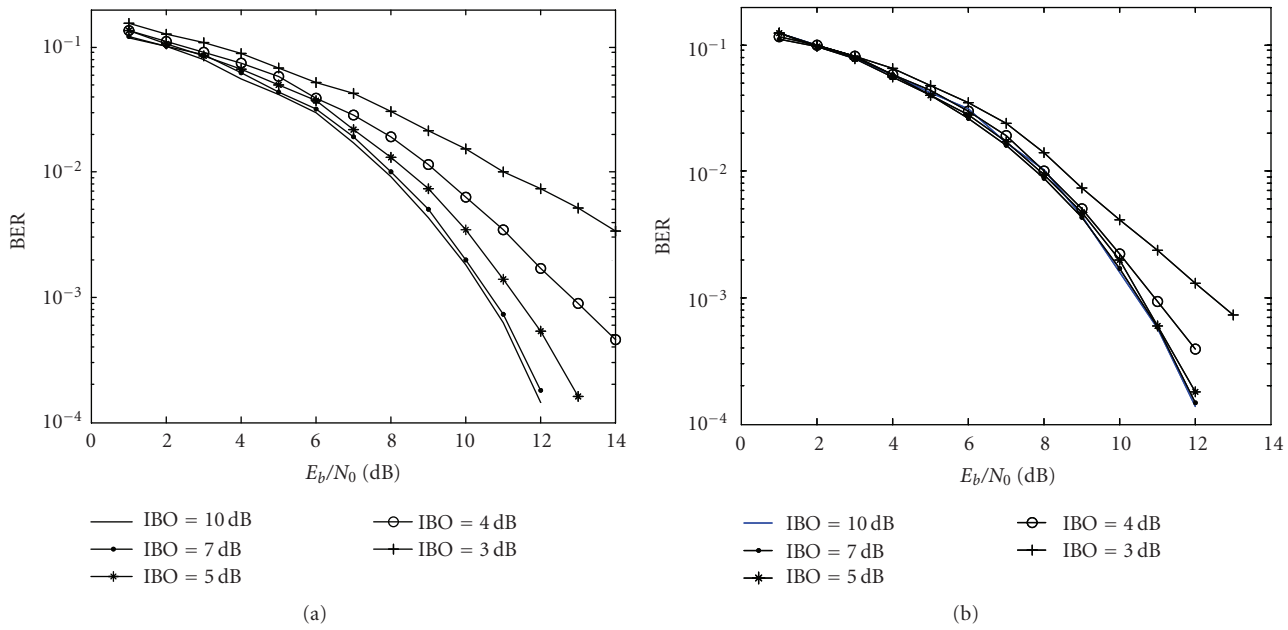

Figure 5: Bit error rate due to additive white Gaussian noise added to 16 QAM serial modulated signals emerging from one stage of clipping and filtering plus an Rapp model nonlinearity. (a) Rapp parameter $p = 2$; (b) Rapp parameter $p = 10$. Clipping level equals amplifier saturation level. (IBO = power backoff in dB.)

regrowth due to $p = 2$ and $p = 10$ nonlinearities are shown in Figures 6(a) and 6(b), respectively, for QPSK serial modulation and OFDM signals. The backoffs required to achieve the same output spectra as those of Figures 3(a) and 4(a) have *not* been significantly reduced for $p = 2$ as a result of applying clipping and filtering. For $p = 10$, backoffs have been reduced by less than 1 dB for both serial modulation and OFDM. The signal-to-nonlinear distortion ratio is below 33 dB for each of these cases. Thus, reductions in backoff from clipping and filtering are seen to be only significant when combined with an HPA which has been linearized (corresponding to a high value of p).

5. MODIFIED SLM ALGORITHM

Selective mapping (SLM) is a recognized method for PAPR reduction in OFDM signals [17]. This method is based on generating N_s different transformed blocks for each given block of data. Then, it transmits the one with the lowest PAPR and some side information to the receiver about the identity of the transform of the block. In the conventional SLM method, to generate independent blocks of data, each block is multiplied symbol by symbol, before the IFFT operation, by one of the pseudorandom but fixed sets of vectors whose elements are complex numbers with unit amplitude and a random phase uniformly distributed between $[0, 2\pi]$. In contrast to clipping and filtering, SLM introduces no extra distortion to the signal that is to be amplified by the HPA.

In SLM-OFDM, the transmitter selects the signal with the lowest peak as the best one. In SM, high peaks are generated after filtering, when there are large magnitude points of the constellation near each other in the data sequence. Consequently, the number of large peaks in an SM block is greater than that of OFDM. This makes the distribution of the amplitude in SM different from OFDM. A modified version of the SLM algorithm for SM is suggested in [10]. The proposed method has two differences from the original SLM. The first one is the method of generating random blocks and the second one is the selection rule.

In the suggested SLM method, like OFDM, N_s different blocks of data are generated in the transmitter, but each one is a permuted version of the original sequence to avoid occurrence of consecutive high peaks. Therefore, the transmitter does not need the pseudorandom sequence, and the side information only determines the selected permutation for the receiver. The permuted signal with the smallest mean squared error between the input signal and the output signal of the nonlinear amplifier is chosen for transmission. The metric which is based on the sum of squared errors (SSEs) is

$$m_k = \sum_{n=0}^{N-1} \left| e_k(n) \right|^2, \quad 1 \le k \le N_s, \tag{11}$$

where

$$e_k(n) = \begin{cases} \left| V_{\text{in},k}(n) \right| - .9\, V_{\text{sat}}, & \left| V_{\text{in},k}(n) \right| \ge .9 V_{\text{sat}}, \\ 0, & \text{otherwise}, \end{cases} \tag{12}$$

and k is the index of each permutation and N is the number of samples per data block.

The system requires transmitting $\log_2 N_s$ bits as side information for each data block which is the same as the required side information for the SLM-OFDM method. Simulation results show that this method considerably improves

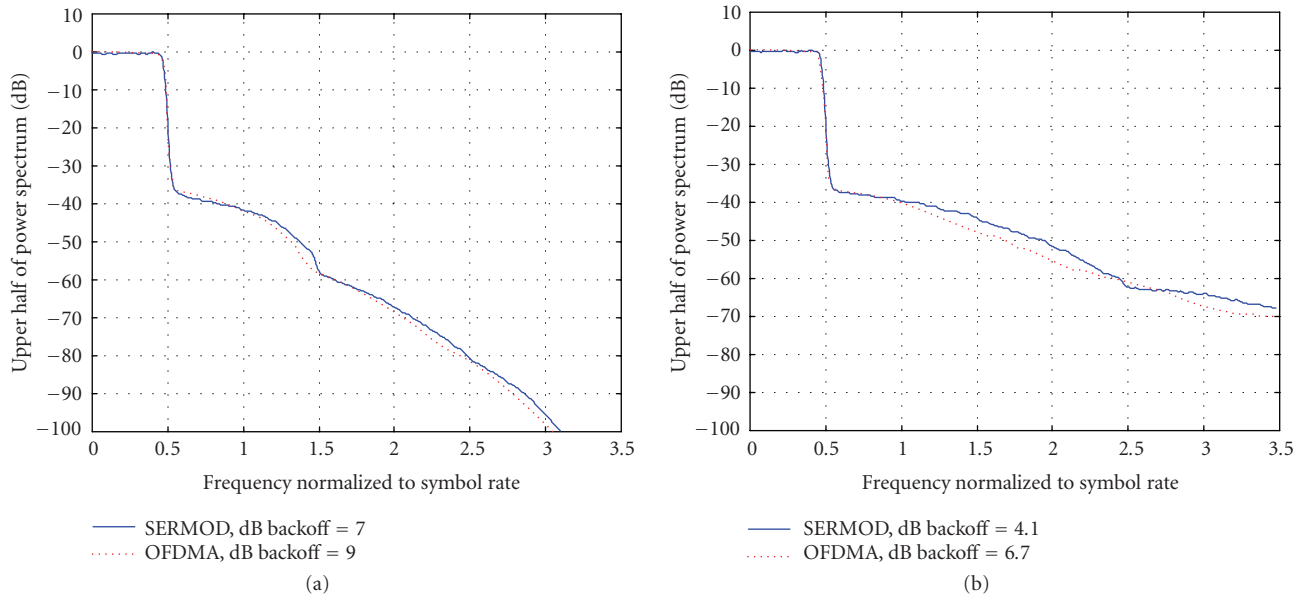

FIGURE 6: Output power spectra of QPSK signals with 4 iterations of clipping and filtering passed through an Rapp model nonlinearity with parameter (a) $p = 2$, (b) $p = 10$.

the envelope distribution and reduces the out-of-band radiation. In all of the simulations, the transmitted blocks contain 256 symbols randomly chosen from a 16-QAM constellation. Raised-cosine time-domain windowing is used. The transmitter generates $N_s = 4$ blocks for each data block in the SLM method. Out-of-band radiations of SM and OFDM are depicted in Figures 7(a) and 7(b). In both figures, we considered power backoffs of 5 and 7 dB for an amplifier with $p = 10$ and backoff of 5 dB for $p = 2$. SLM can significantly decrease the out-of-band components which cause interference for other subscribers using these frequencies, especially the first sidelobe. We note that, for a given power backoff, SLM is more effective for an amplifier with larger Rapp parameter p which is more linear up to the saturation level. Thus, SLM, like other PAPR-reduction methods, is most effective when used with an HPA that approximates an ideal linear clipper, or whose input-output characteristic is compensated by an adaptive predistortion scheme. The work in [11] describes a variation of this PAPR reduction method applied to MC-CDMA and serial CDMA.

6. GMC SIGNALS WITH NONCONTIGUOUS DATA SPECTRA

For the purpose of channel estimation for frequency domain equalizer adaptation, pilot training signals are usually multiplexed with data signals in some or all transmitted OFDM symbols. If they are time-multiplexed via separate short training blocks, there is no implication for PAPR or power backoff, as long as the training signals have uniform amplitude, such as Chu sequences [25]. However, pilots frequency-multiplexed with data can affect PAPR properties of the resulting composite signal. A common form of frequency-multiplexed pilots is inserted with a *frequency expanding technique* (FET). In this technique, rows of zeroes are periodically inserted in the **F** matrix in (4) in case of DFT-precoded OFDM, or in the identity matrix in **M** in case of OFDM. Thus, pilot tones appear at uniformly spaced frequencies in the transmitted spectrum, surrounded by data-carrying tones. The pilot tones can be chosen to be DFT components of a Chu sequence, so that the power spectrum and amplitude samples of the pilot waveform are uniform [26, 27]. A length-L Chu sequence can be obtained by

$$c_n = \begin{cases} e^{j\pi q n^2/L} & \text{for } L \text{ even}, \\ e^{j\pi q n(n+1)/L} & \text{for } L \text{ odd}, \end{cases} \tag{13}$$

where q is relatively prime to L, and $n = 0, 1, 2, \ldots, L-1$. The FET pilot sequence in the frequency domain is the L-point DFT of $\{c_n\}$. Since the pilot subcarriers are at regular intervals, the added pilot waveform is equivalent to a low-PAPR IFDMA waveform.

For OFDM, there is little or no effect on PAPR properties since pilot tones resemble data tones. However, when FET pilots are applied to DFT-precoded OFDM, the resulting time-domain sampled data waveform (not including the pilot waveform) can be shown to be [26]

$$s(n) = \sum_{m=0}^{M-1} a_m g_1\left(n - m\frac{N}{M}\right) g_2\left(n - m\frac{NK}{(K+1)M}\right), \tag{14}$$

where K is the interpilot spacing, and

$$g_1(n) = \frac{1}{\sqrt{M}} e^{j(\pi/N)(K-1)n} \frac{\sin((\pi K/N)n)}{\sin((\pi/N)n)},$$
$$g_2(n) = \frac{1}{\sqrt{M}} e^{j(\pi/N)(K+1)((M/K)-1)n} \frac{\sin((\pi(K+1)M/NK)n)}{\sin((\pi(K+1)/N)n)}. \tag{15}$$

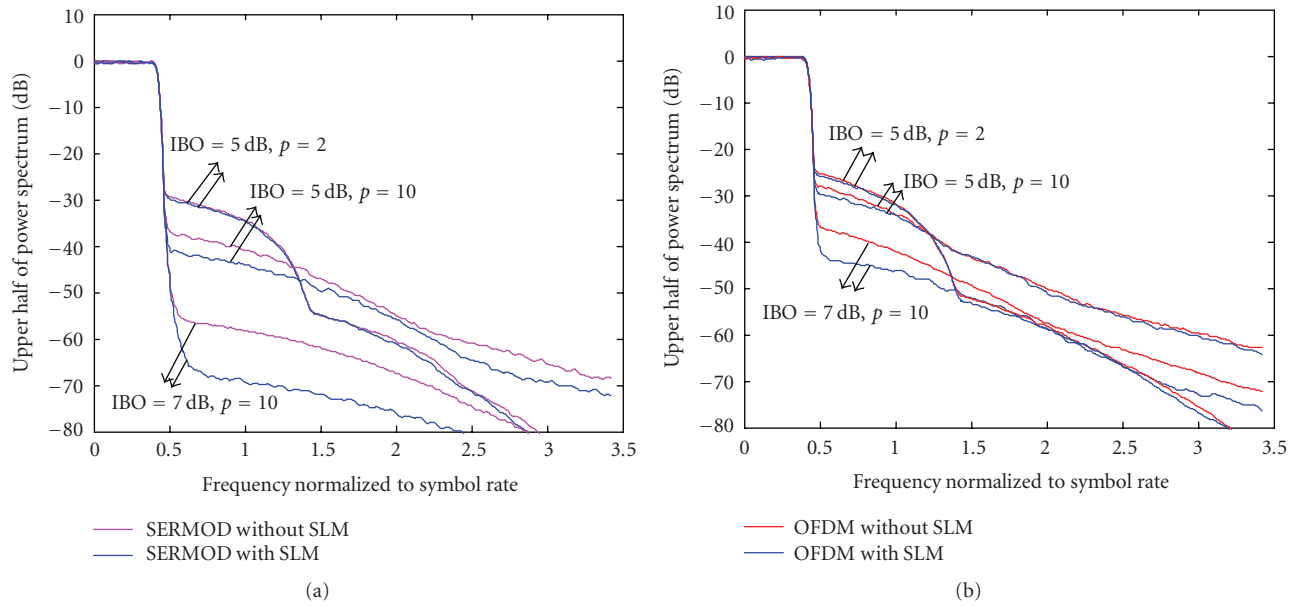

FIGURE 7: Reduction of spectral sidelobes by SLM for (a) 16 QAM *serial modulation*; (b) 16 QAM *OFDM*; (IBO = backoff in dB, p = Rapp parameter p).

This is no longer a pure serial modulated waveform, and so it can be expected that its amplitude range properties will be worse than those of the SM waveform of (5). Furthermore, the pilot waveform is added to it.

Figure 8 shows double-sided QPSK DFT-precoded SM and OFDM spectra at the output of Rapp $p = 2$ nonlinearity, along with a spectral mask that has been proposed for WINNER wireless systems [28]. The frequency axis in this figure is normalized to the proposed WINNER channel spacing instead of the symbol rate. The signals are of the same type as those of Figure 3(a), but they have FET pilots inserted at every 4th subcarrier. The OFDM spectrum and backoff to satisfy the mask are nearly identical to those of Figure 3(a), but the serial modulated signal with FET pilots requires about 1 dB higher backoff although it is still 1 dB less than that of the OFDM signal. Typical pilot arrangements will place pilots in only a fraction of the transmitted blocks, for example, in 2 blocks out of 12 as in [26]. Thus, only a fraction of transmitted SM blocks needs the slight extra backoff associated with FET pilots. For those blocks, the pilot level can be boosted slightly and the data power can be decreased, the only effect being a fraction of dB loss in average data signal SNR [27]. In Figure 8, the pilot power has been boosted by 1 dB for the SM signal, and the resulting SNR loss to data, if 1/6 of transmitted blocks has pilots, is 0.2 dB.

Figure 9 shows spectral regrowth plots for IFDMA and B-IFDMA signals mentioned in Section 2, and further detailed in [23]. In both plots, the number of used subcarriers is 128, and the nominal bandwidth is 40 MHz. The spacing between adjacent blocks of occupied subcarriers is 8 subcarriers for IFDMA and 32 subcarriers for B-IFDMA. Even though the B-IFDMA waveform is not a pure SM waveform, its backoff is less than that of the OFDMA signal, and it is only slightly larger than that of IFDMA.

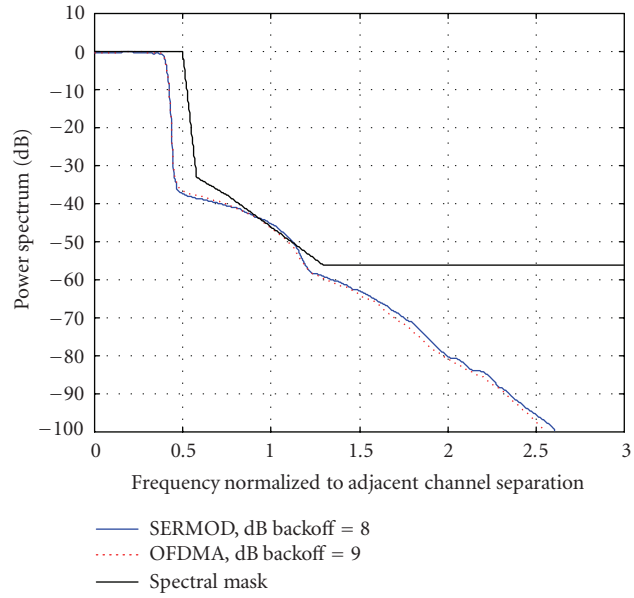

FIGURE 8: Power spectra for $p = 2$ Rapp model nonlinearity for QPSK serial modulated and OFDM signals, with FET pilot tone at every 4th subcarrier. Also shown is a spectral mask proposed for WINNER systems.

The work in [29] proposed a method of reducing the PAPR for OFDM signal by selecting the pilot sequence from a number of possible orthogonal Walsh-Hadamard pilot sequences, such that the OFDM signal with pilots gives the lowest PAPR. As shown in [29], the use of orthogonal pilot sequences facilitates blind detection of which pilot sequence has been sent, by the receiver, so that no side information

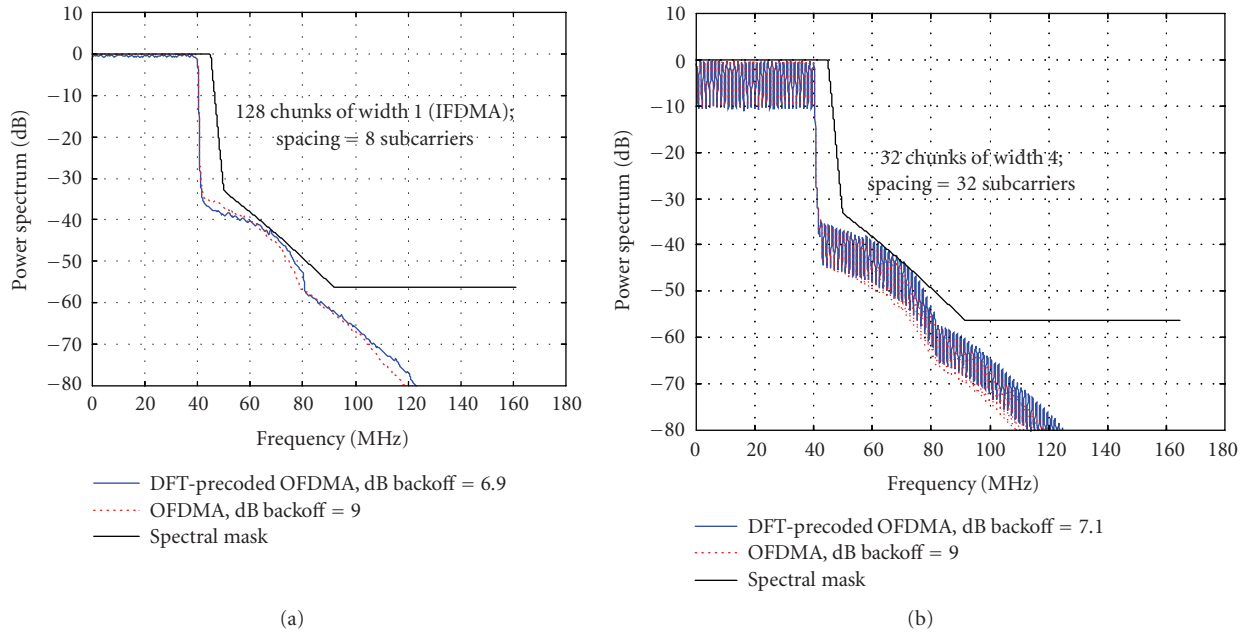

Figure 9: HPA output power spectra for OFDMA and DFT-precoded OFDMA. (a) IFDMA with 128 subcarriers, block width = 1, and 8-subcarrier spacing between subcarriers; (b) B-IFDMA with 128 subcarriers, block width = 4, and 32-subcarrier spacing between blocks. Both are with 40 MHz nominal bandwidth. HPA has Rapp model nonlinearity with parameter $p = 2$.

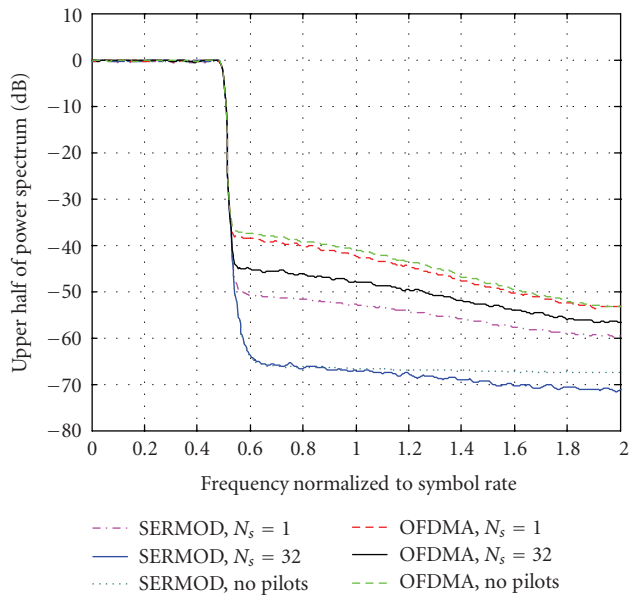

Figure 10: Power spectra of QPSK DFT-precoded and OFDM signals with $M = 416$ data symbols/block and 104 FET pilots formed from one of the N_s cyclically shifted Chu sequences chosen to minimize PAPR. Rapp parameter $p = 10$; backoff = 7 dB.

is necessary. The work in [9] extends this concept to DFT-precoded OFDM signals, using orthogonal cyclically shifted Chu pilot sequences instead of Walsh-Hadamard sequences, and using either a PAPR selection rule as in [29] or the SSE selection rule of [10]. Figure 10 shows power spectra from the output of a $p = 10$ Rapp nonlinearity, using this cyclically shifted Chu pilot sequence selection technique, with power backoff of 7 dB, for both DFT-precoded OFDM and OFDM signals. The parameter N_s is the number of Chu pilot sequences from which the PAPR-minimizing selection is made. Results for the SSE rule are similar [9]. $N_s = 1$ corresponds to conventional FET pilots with no PAPR reduction applied. Every 4th subcarrier is a pilot. Choosing from $N_s = 32$ possible pilot sequences is seen to reduce sidelobe regrowth slightly for the serial modulation case, even showing improvement over the case of no pilots. The improvement over the case of no pilots is more significant for OFDM. However, for the case where 1/4 of the occupied subcarriers is pilots, the sidelobe reduction obtained by choosing among $N_s = 32$ pilot sequences is more significant for DFT-precoded signals than for OFDM signals. Again, however, the improvement is only significant for the linear clipper ($p = 10$) HPA model; there is little improvement for $p = 2$ [9].

In [13], this idea is carried further, by combining it with the SLM procedure; each possible pilot sequence based on the selected codeword of a maximum length code is combined with a different SLM mask sequence. The mask/pilot combination giving the least PAPR is chosen at the transmitter.

7. HPA PREDISTORTION METHODS

We have seen that the required power backoff is significantly reduced, and the effectiveness of PAPR reduction methods is significantly enhanced if the HPA nonlinearity resembles that of an ideal linear clipper (e.g., for Rapp parameter $p = 10$). A means to achieve this desirable HPA characteristic is to predistort the HPA input signal (after any PAPR reduction

techniques have been applied) with a nonlinear circuit having a characteristic that is reciprocal to the HPA characteristic. A lookup table (LUT) can be applied to store the value of a variable complex gain which depends on the current value of the input signal magnitude. The size of the LUT is determined by the quantization accuracy of the input signal magnitude. The adaptation algorithm modifies the contents of each memory cell which has to be selected by the input signal. OFDM waveforms have an approximately Gaussian distribution, and hence some of the memory cells are very rarely addressed and their contents are rarely modified. This results in a slow convergence of the HPA predistortion process. The speed of convergence of the adaptation algorithm can be increased [30].

Instead of applying a predistorter based on a variable gain retrieved from the LUT, HPA reciprocal characteristics can be adaptively synthesized using a small number of nonlinear elements. In [31], the results of neural networks applied to the HPA compensation have been reported proving their good performance for predistorters both with and without memory. It has been also proved in [32] that a predistorter based on memory polynomials (another example of the nonlinear "elements") results in much more effective HPA nonlinearity compensation than that which operates on the current signal only.

Another predistortion algorithm based on the principle of piecewise linear approximation of the HPA inverse characteristics is evaluated in [12, 33]. Recall that in case of solid-state amplifiers, the AM/PM conversion is negligible, therefore only the AM/AM HPA characteristics have to be compensated.

As in the LUT-based predistorter, the baseband signal in form of the in-phase and quadrature components is converted into polar form. Only the signal magnitude is a subject of processing by the predistorter. First, the piecewise characteristic which compensates for the inverse HPA characteristic has to be selected. In order to do this, the range of the input signal magnitudes is divided into smaller M_s subranges. In this way, the x-coordinates of the break points of the piecewise linear function are chosen. The adaptation algorithm finds the best y-coordinates of these points such that for a given signal block the mean square error of the following form is minimized:

$$C = \sum_{k=1}^{M_s} \sum_{i=1}^{n_k} \left(A\left(y_k^{(i)}\right) - x_k^{(i)}\right)^2 = \sum_{k=1}^{M_s} \sum_{i=1}^{n_k} \left(e_k^{(i)}\right)^2, \tag{16}$$

where n_k is the number of samples contained in the kth range of the predistorter signal, $x_k^{(i)}$ is the ith sample of predistorter input signal belonging to the kth subrange, $y_k^{(i)}$ is the ith sample of the predistorter output signal belonging to the kth subrange, (x_k, y_k) are the coordinates of the kth knee-points of the predistorter characteristics, and $A(\cdot)$ is the HPA AM/AM characteristic.

We note that the total number of signal samples on which predistorter optimization is based is equal to

$$n = \sum_{k=1}^{M_s} n_k, \tag{17}$$

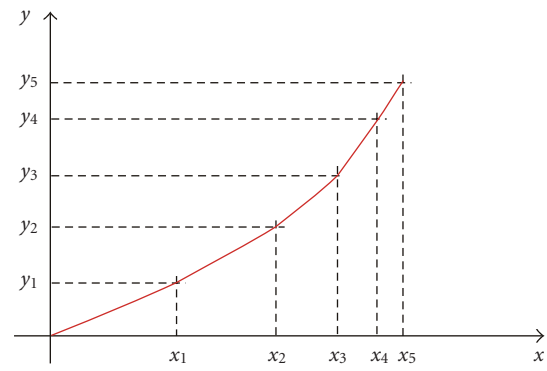

Figure 11: Piecewise linear AM/AM characteristics of the predistorter.

and it is, for example, the number of samples representing a single OFDM symbol or a single block of a GMC signal.

Figure 11 presents the approximation of the AM/AM characteristic of the predistorter. At the given x-coordinates of the knee-points, their y-coordinates are adjusted to minimize the mean square error on the output of the HPA. The error is given by the expression

$$e_k^{(i)} = A\left(y_k^{(i)}\right) - x_k^{(i)}. \tag{18}$$

Let us recall that due to the applied piecewise linear approximation, the y-coordinates of the characteristics belonging to the neighboring kth and $(k+1)$th subranges are described by the formulas

$$\begin{aligned} y_k^{(i)} &= \frac{y_k - y_{k-1}}{x_k - x_{k-1}}\left(x_k^{(i)} - x_{k-1}\right) + y_{k-1}, \\ y_{k+1}^{(i)} &= \frac{y_{k+1} - y_k}{x_{k+1} - x_k}\left(x_{k+1}^{(i)} - x_k\right) + y_k. \end{aligned} \tag{19}$$

In order to adjust the y-coordinates $y_k (k = 1, \ldots, M_s)$ adaptively, the gradient of the cost function C is calculated:

$$\frac{\partial C}{\partial y_k} = \sum_{i=1}^{n_k} 2e_k^{(i)} \frac{\partial e_k^{(i)}}{\partial y_k} + \sum_{i=1}^{n_{k+1}} 2e_{k+1}^{(i)} \frac{\partial e_{k+1}^{(i)}}{\partial y_k}. \tag{20}$$

Calculation of the partial derivatives in the above formula leads to the following results:

$$\frac{\partial e_k^{(i)}}{\partial y_k} = \frac{\partial A(y)}{\partial y}\Big|_{y=y_k^{(i)}} \frac{x_k^{(i)} - x_{k-1}}{x_k - x_{k-1}}, \tag{21}$$

$$\begin{aligned} \frac{\partial e_{k+1}^{(i)}}{\partial y_k} &= \frac{\partial A(y)}{\partial y}\Big|_{y=y_{k+1}^{(i)}} \left[1 - \frac{x_{k+1}^{(i)} - x_k}{x_{k+1} - x_k}\right] \\ &= \frac{\partial A(y)}{\partial y}\Big|_{y=y_{k+1}^{(i)}} \frac{x_{k+1} - x_{k+1}^{(i)}}{x_{k+1} - x_k}. \end{aligned} \tag{22}$$

Using the following approximation of derivatives:

$$\frac{\partial A(y)}{\partial y}\Big|_{y=y_k^{(i)}} \approx \frac{x_k - x_{k-1}}{y_k - y_{k-1}}, \qquad \frac{\partial A(y)}{\partial y}\Big|_{y=y_{k+1}^{(i)}} \approx \frac{x_{k+1} - x_k}{y_{k+1} - y_k} \tag{23}$$

in (22), applying (20), and performing some mathematical simplifications, we obtain the expression describing the predistorter adaptation algorithm for the jth OFDM symbol:

$$y_{k,j+1} = y_{k,j} - \alpha_k \left\{ \frac{1}{y_{k,j} - y_{k-1,j}} \sum_{i=1}^{n_k} e_k^{(i)} \left(x_k^{(i)} - x_{k-1}\right) - \frac{1}{y_{k+1,j} - y_{k,j}} \sum_{i=1}^{n_k} e_{k+1}^{(i)} \left(x_{k+1}^{(i)} - x_k\right) \right\}, \quad k = 1, \ldots, M_s, \tag{24}$$

where α_k is the adaptation step of the algorithm.

Note that the basic part of the iterative adaptation algorithm is the set of M_s correlators which correlate the HPA output error with the difference of the input signal and the x-coordinate of the left edge of the range into which the input signal sample falls.

Note that a similar idea of linear approximation of the signal samples falling between discrete points of the predistorter characteristics was already presented in [34]. Karam and Sari applied it in the LUT predistorter to the in-phase and quadrature serially modulated signal components in order to save the LUT memory size, or equivalently to reduce the number of LUT address bits. Our approach differs not only in the aim of linear approximation but also in the possibility of selection of the predistorter characteristic's knee-points in any locations on the signal magnitude axis which best fit the predistortion goal. We show that the number of knee-points can in practice be very low. We also show the predistorter adaptation algorithm which is integrated with the proposed predistorter structure that has not been discussed in [34].

Let us note that the proposed predistorter based on piecewise approximation of the HPA inverse characteristics and the adaptation algorithm associated with it (represented by (19) and (24)) can be easily implemented digitally. Such a predistorter will produce its output signal at the frequency resulting from the sampling frequency applied in PAPR reduction process.

In order to evaluate the quality of the proposed predistorter algorithm, simulations were performed. Their results for the OFDM signals are shown in Figure 12. The OFDM signal was the sum of 1664 16-QAM modulated subcarriers. The predistorter characteristics consisted of $M_s = 9$ linear segments. The y-coordinates of the knee-points were updated once per each OFDM symbol. As we see, 300 OFDM symbols are sufficient to achieve a good convergence of the predistorter.

Similar results of HPA nonlinearity compensation were achieved when a single-carrier modulation was investigated. As previously, the Rapp model with $p = 2$ was used to simulate the influence of a nonlinear HPA. We simulated serial 16-QAM transmission with spectral shaping by a square-root raised-cosine filter with the rolloff factor being equal to 0.2. Four samples per modulation period were generated. Small sidelobes of the power density spectrum of the generated QAM signals are seen in Figure 13. They result from the shaping filter design exclusively and would be lower if higher-order FIR shaping filter was applied. Despite the nonconstant envelope of a QAM signal with the shaped baseband pulse, its dynamic range is much lower than that of the OFDM signal. Thus, a lower value of IBO can be applied in the HPA. We report our simulations for IBO = 5 dB, although other IBO values were also tested. Figure 13 presents the power density spectrum at the output of the HPA after 0, 50, 100, and 150 iterations of the predistorter adaptation algorithm. The piecewise linear characteristic was adjusted after transmission of each block of 1024 16-QAM symbols. It was found that for IBO = 5 dB, the step size $\alpha_k = 1$ resulted in the fast convergence of the adaptation algorithm. It was also observed that when IBO was lower, the step size had to be decreased as well. As we observe in Figure 13, only 50 iterations of the adaptation algorithm are sufficient to suppress the nonlinear distortion below 40 dB. After 100 iterations, the performance of the HPA with the predistorter is already very good.

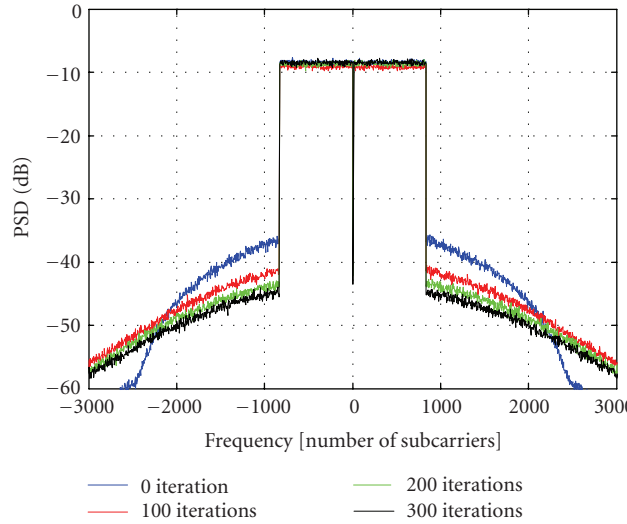

Figure 12: Power spectral density (PSD) on the output of the linearized HPA after operation of the proposed adaptation algorithm for OFDM signals with 1664 16-QAM modulated subcarriers.

8. SUMMARY AND CONCLUSIONS

In general, transmitted signal power spectra must be confined within spectral masks which are designed to prevent excessive out-of-band interference to adjacent channel users. Some power backoff is necessary to keep spectral regrowth due to nonlinear HPAs within the mask limit. We have extended some popular peak power reduction schemes to the class of generalized multicarrier signals, including ones with noncontiguous spectra and with added frequency-multiplexed pilots, showing resulting power backoff reductions. Generally, power backoff requirements must be assessed with respect to specific power amplifier models.

We can summarize by listing the following conclusions.

(1) Most spectral masks for licensed interference-limited wireless systems are such that as long as they are not violated, in-band distortion and BER degradation due to

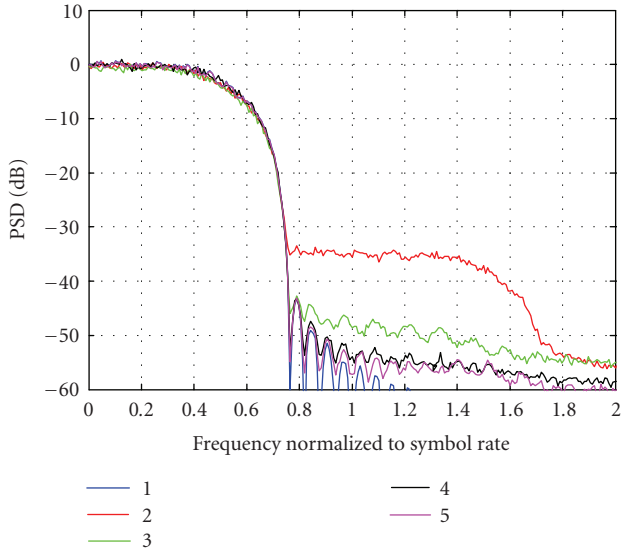

FIGURE 13: (1) PSD on the output of the linear amplifier and (2) the nonlinear amplifier before predistorter adaptation (3) after 50 iterations, (4) 100 iterations, and (5) 150 iterations of the predistorter adaptation algorithm for single-carrier 16-QAM modulated signal blocks with the square-root raised-cosine shaping filter (rolloff factor equal to 0.2).

HPA nonlinearity are negligible. This means that spectral regrowth is a more important criterion than BER when assessing nonlinear HPA effects.

(2) Required power backoff for a specific HPA nonlinearity model and spectrum mask is a better *quantitative* criterion than peak-to-average power ratio or its distribution.

(3) DFT-precoded OFDM has lower PAPR and lower backoff requirements than OFDM or OFDMA. It is equivalent to serial or single-carrier modulation if the transmitted subcarriers are contiguous or equally spaced. DFT precoding can in fact be considered as an effective PAPR reduction technique for OFDM.

(4) Several other PAPR reduction schemes, that have been previously found to be effective for OFDM, are also effective for DFT-precoded OFDM, in particular, SLM, pilot-selection schemes, and, perhaps surprisingly, clipping and filtering. However, when used for reducing required power backoff, these schemes are most effective when combined with adaptive HPA predistortion which effectively makes the HPA nonlinear characteristic close to that of an ideal linear clipper.

(5) A novel piecewise linear HPA predistortion technique, with a few well-chosen knee-points, was described and found effective in reducing the out-of-band spectrum.

ACKNOWLEDGMENTS

This work has been performed in the framework of the IST Project, IST-4-027756 WINNER, which is funded by the European Union. This work was partly funded by the WINNER Project and the Natural Sciences and Engineering Research Council (NSERC) of Canada. The authors would like to acknowledge the contributions of their colleagues in WINNER, although the views expressed are those of the authors and do not necessarily represent the project.

REFERENCES

[1] P. Struhsaker and K. Griffin, "Analysis of PHY Waveform Peak to Mean Ratio and Impact on RF Amplification," contribution to IEEE 802.16.3c-01/46, March 2001.

[2] B. Come, S. Donnay, L. Van der Perre, et al., "Impact of front-end non-idealities on bit error rate performance of WLAN-OFDM transceivers," in *Proceedings of IEEE Radio and Wireless Conference (RAWCON '00)*, pp. 91–94, Denver, Colo, USA, September 2000.

[3] M. Lampe and H. Rohling, "Reducing out-of-band emissions due to nonlinearities in OFDM systems," in *Proceedings of IEEE Vehicular Technology Conference (VTC '99)*, vol. 3, pp. 2255–2259, Houston, Tex, USA, July 1999.

[4] S. H. Han and J. H. Lee, "An overview of peak-to-average power ratio reduction techniques for multicarrier transmission," *IEEE Wireless Communications*, vol. 12, no. 2, pp. 56–65, 2005.

[5] Z. Wang and G. B. Giannakis, "Wireless multicarrier communications," *IEEE Signal Processing Magazine*, vol. 17, no. 3, pp. 29–48, 2000.

[6] D. Falconer and S. Kaiser, Eds, "Broadband Frequency Domain-Based air Interfaces for Future-Generation Wireless Systems," WWRF WG4 White paper, September 2005, http://wg4.ww-rf.org/WWRF_WG4_FD_air_interface_WP.doc.

[7] R. TafazolliEds, *Technologies for the Wireless Future*, John Wiley & Sons, New York, NY, USA, 2006.

[8] C. Liu, H. Xiao, Q. Wu, and F. Li, "System design of RF power amplifiers for wireless communication systems," *IEEE Transactions Consumer Electronics*, vol. 48, no. 1, pp. 72–80, 2002.

[9] C.-T. Lam, D. Falconer, and F. Danilo-Lemoine, "PAPR reduction using frequency domain multiplexed pilot sequences," in *Proceedings of IEEE Wireless Communications and Networking Conference (WCNC '02)*, pp. 1428–1432, Hong Kong, March 2007.

[10] M. Sabbaghian and D. Falconer, " Reducing required power back-off of nonlinear amplifiers in serial modulation using SLM method," in *Proceedings of the 62nd IEEE Vehicular Technology Conference (VTC '05)*, vol. 3, pp. 1882–1886, Dallas, Tex, USA, September 2005.

[11] M. Sabbaghian and D. Falconer, "Peak to average power ratio properties of MC-CDMA and SM-CDMA," in *Proceedings of the 63rd IEEE Vehicular Technology Conference (VTC '06)*, vol. 4, pp. 2013–2017, Melbourne, Australia, May 2006.

[12] K. Wesołowski, "A novel fast HPA predistorter for high PAPR signals," in *Proceedings of IEEE International Symposium on Personal, Indoor and Mobile Radio Communications (PIMRC '05)*, vol. 2, pp. 863–867, Berlin, Germany, September 2005.

[13] K. Wesołowski, "On the PAPR minimization using selected mapping algorithm in pilot-assisted OFDM systems," in *Proceedings of European Wireless*, Paris, France, April 2007.

[14] A. E. Jones, T. A. Wilkinson, and S. K. Barton, "Block coding scheme for reduction of peak to mean envelope power ratio of multicarrier transmission schemes," *Electronics Letters*, vol. 30, no. 25, pp. 2098–2099, 1994.

[15] A. E. Jones and T. A. Wilkinson, "Combined coding for error control and increased robustness to system nonlinearities in

OFDM," in *Proceedings of the 46th IEEE Vehicular Technology Conference (VTC '96)*, vol. 2, pp. 904–908, Atlanta, Ga, USA, May 1996.

[16] L. J. Jr. Cimini and N. R. Sollenberger, "Peak to average power reduction of an OFDM signal using partial transmit sequences," *IEEE Communications Letters*, vol. 4, no. 3, pp. 86–88, 2000.

[17] S. H. Muller and J. B. Huber, "A novel peak power reduction scheme for OFDM," in *Proceedings of the 8th IEEE International Symposium on Personal, Indoor and Mobile Radio Communications (PIMRC '97)*, vol. 3, pp. 1090–1094, Helsinki, Finland, September 1997.

[18] S. Sezginer and H. Sari, "OFDM peak power reduction with simple amplitude predistortion," *IEEE Communications Letters*, vol. 10, no. 2, pp. 65–67, 2006.

[19] J. Armstrong, "Peak-to-average power reduction for OFDM by repeated clipping andfrequency domain filtering," *Electronics Letters*, vol. 38, no. 5, pp. 246–247, 2002.

[20] R. Dinis and A. Gusmão, "A class of nonlinear signal-processing schemes for bandwidth-efficient OFDM transmission with low envelope fluctuation," *IEEE Transactions on Communications*, vol. 52, no. 11, pp. 2009–2018, 2004.

[21] H. Ochiai, "Power efficiency comparison of OFDM and single-carrier signals," in *Proceedings of the 56th IEEE Vehicular Technology Conference (VTC '02)*, vol. 2, pp. 899–903, Vancouver, Canada, September 2002.

[22] R. Dinis, D. Falconer, C.-T. Lam, and M. Sabbaghian, "A multiple access scheme for the uplink of broadband wireless systems," in *Proceedings of IEEE Global Telecommunications Conference (GLOBECOM '04)*, vol. 6, pp. 3808–3812, Dallas, Tex, USA, December 2004.

[23] T. Svensson, T. Frank, D. Falconer, M. Sternad, E. Costa, and A. Klein, "B-IFDMA—a power-efficient multiple access scheme for non-frequency-adaptive transmission," in *Proceedings of the16th IST Summit Conference*, pp. 1–5, Budapest, Hungary, July 2007.

[24] C. Rapp, "Effects of HPA nonlinearity on a 4DPSK/OFDM signal for a digital sound broadcasting system," in *Proceedings of the 2nd European Conference on Satellite Communications*, pp. 179–184, Liege, Belgium, October 1991.

[25] D. C. Chu, "Polyphase codes with good periodic correlation properties," *IEEE Transactions on Information Theory*, vol. 18, no. 4, pp. 531–532, 1972.

[26] C.-T. Lam, D. Falconer, F. Danilo-Lemoine, and R. Dinis, "Channel estimation for SC-FDE systems using frequency domain multiplexed pilots," in *Proceedings of the 64th IEEE Vehicular Technology Conference (VTC '06)*, pp. 1438–1442, Montreal, Canada, September 2006.

[27] C.-T. Lam, G. Auer, F. Danilo-Lemoine, and D. Falconer, "Design of time and frequency domain pilots for generalized multicarrier systems," in *Proceedings of IEEE International Conference on Communications (ICC '07)*, pp. 4076–4081, Glasgow, Scotland, June 2007.

[28] IST-2003-507581 WINNER, "Duplex Arrangements for Future Broadband Radio Interface," October 2004.

[29] M. Garca, O. Edfors, and J. Paez-Borrallo, "Peak power reduction for OFDM systems with orthogonal pilot sequences," *IEEE Transactions on Wireless Communications*, vol. 5, no. 1, pp. 47–51, 2006.

[30] K. Wesołowski and J. Pochmara, "Efficient algorithm for adjustment of adaptive predistorter in OFDM transmitter," in *Proceedings of the 53rd IEEE Vehicular Technology Conference (VTC '01)*, vol. 5, pp. 2491–2496, Boston, Mass, USA, September 2000.

[31] J. Pochmara, "Improving compensation of nonlinear distortions in OFDM system using recurrent neural network with conjugate gradient algorithm," in *Proceedings of the 15th IEEE International Symposium on Personal, Indoor and Mobile Radio Communications (PIMRC '04)*, vol. 1, pp. 180–185, Barcelona, Spain, September 2004.

[32] L. Ding, G. T. Zhou, D. R. Morgan, Z. Ma, J. S. Kenney, J. Kim, and Ch. Giardina, "A robust digital baseband predistorter constructed using memory polynomials," *IEEE Transactions on Communications*, vol. 52, no. 1, pp. 159–165, 2004.

[33] IST-2003-507581 WINNER, "D2.3 Assessment of Radio-Link Technologies," February 2005.

[34] G. Karam and H. Sari, "Generalized data predistortion using intersymbol interpolation," *Philips Journal of Research*, vol. 46, no. 1, pp. 1–22, 1991.